Scattering of evanescent and radiative fields of a Gaussian beam by a perfect electromagnetic conductor cylinder

ABDUL GHAFFAR[a,b], MAJEED A. S. ALKANHAL[a]
[a] Department of Electrical Engineering, King Saud University, Saudi Arabia
[b]Department of Physics, University of Agriculture, Faisalabad, Pakistan

The scattering of a Gaussian beam by a perfect electromagnetic conductor (PEMC) cylinder is analyzed using plane wave spectrum method. The PEMC material is characterized by a single parameter M, whose zero and infinite value-limits reduce to the perfect magnetic conductor (PMC) and the perfect electric conductor (PEC), respectively. The presented analysis examined the effect of the evanescent beam in the total scattering. It is found that an evanescent wave scatters from the PEMC cylinder and partially converted into radiation. The effects of the scattering angle, the admittance parameter, and the beam width of the Gaussian beam on the co-polarized and the cross-polarized components of the scattered fields have been explained. The obtained results for the cases of $M \to \infty$ (PEC) and $M = 0$ (PMC) compared very well with the published results. Result comparison with published data for both a Gaussian-beam and a plane-wave incidence is also presented.

1. Introduction

The wave emitted from any electromagnetic source can be divided into radiative and non-radiative fields. The radiation source provide propagating wave which is known to contribute to the far-field as well as to the monostatic or bistatic scattering. The latter provides non-radiating field which is confined in a certain region and cannot be detected outside the region [1]. Information about an object can be obtained locally by the perturbation of the evanescent fields [2]. This has been used effectively in near field microscopy and near field optics [3]. These waves decay exponentially away from the origin. When evanescent waves scatter from small particles, part of their energy can be converted into radiation. In microwave region, investigating the perturbation of evanescent fields helps to have a better antenna arrangement, to detect objects buried underground or to improve the resolution in microwave imaging, among other applications.

The problem of scattering of an incident plane wave by a conducting cylinder, have been extensively studied [4-7] and further extended to scattering of a Gaussian beam instead of a simple plane wave due its extra practical importance [8]. Many researchers carried out the study of the scattering of a Gaussian beam by conducting cylinders and spheres [9-11]. Gaussian beam scattering from a dielectric cylinder including the evanescent region [12] and evanescent wave impedance and scattering conversion into radiation by the same authors have been presented in the literature [13] while the more complex problem of scattering of electromagnetic radiations from PEMC cylinder

including evanescent region has not been yet presented in the literature. The contribution of the evanescent region has been overlooked by several authors.

The generalization of the perfect electric conductors (PEC) and perfect magnetic conductors (PMC) as perfect electromagnetic conductors (PEMC) by Lindell [14] facilitates the study of the scattering of a defined Gaussian beam rather than the infinitely extended waves by a PEMC cylinder. It has been demonstrated theoretically that a PEMC material acts as a perfect reflector of electromagnetic waves but differs from PEC and PMC in that the reflected waves have a cross polarized component [15]. The boundary conditions at the surface of a PEMC are:

$$\left. \begin{array}{l} n \times (H + ME) = 0 \\ n \cdot (D - MB) = 0 \end{array} \right\} \quad (1)$$

where n is the unit vector normal to the boundary, and M is the admittance parameter characterizing the PEMC. The values $M = 0$ and limit $M \to \pm\infty$, correspond to PMC and PEC respectively.

Scattering of electromagnetic radiation by a perfect electromagnetic conducting cylinder was investigated by R. Ruppen [16]. Other studies relevant to PEMC scattering have been presented by Q.A. Naqvi et.al. [17-19]. In these analysis plane waves, cylindrical waves and spherical waves are assumed as waves produced by the source radar. Under practical and experimental conditions, it is necessary to consider a bounded beam rather than the infinitely extended waves. In this paper, scattering properties of a PEMC cylinder by a Gaussian beam has

been carried out including the evanescent region fields. This analysis reveals the occurrence of cross polarized components in the scattered field. Here we present a theoretical scheme for the analysis of scattering of a Gaussian beam from a PEMC cylinder. The presented analysis and formulations are general for any perfect conductor cylinder (PEC, PMC, or PEMC) into evanescent region. The analysis and computations have been carried to study the effects of scattering angle, admittance parameter, and beam width of the Gaussian beam on the scattered fields by the PEMC cylinder in the radiated and evanescent regions.
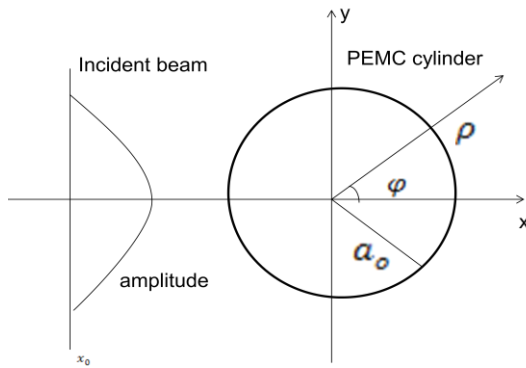
Fig. 1. Geometry of the incident beam and the PEMC cylinder.

2. Expressions for the incident electric field

Consider a PEMC circular cylinder as shown in Fig. 1. The radius of the cylinder is a_0 and it is infinite in length. The source of excitation for the incident beam is located at distance x_0 in the negative x direction from the origin and the far field expression for the incident beam is assumed to be of the following form [4]

$$E_z^i(-x_0, y) = E_0 e^{-\beta^2 y^2} \qquad (2)$$

Here, $\beta^2 = a^2 + jb^2$ and $1/|\beta|$ is the width of the incident beam. We assumed a collimated beam so that $\beta = a$ is taken as real number [5]. For PEC or PMC cylinders, when the polarization of the incident field is parallel to the cylinder axis (TM polarization), the scattered fields are also of the TM type. Similarly, when the incident field polarization is perpendicular to the cylinder axis (TE polarization), the scattered field is purely of the TE type. However, in the general PEMC cylinder case, there also appear cross-polarized components in the scattered fields. For TM polarized incident wave, the Helmholtz wave equation for an incident electric field component in Cartesian coordinates system is given by [4]

$$\frac{\partial^2 E_z^i}{\partial x^2} + \frac{\partial^2 E_z^i}{\partial y^2} + k^2_0 E_z^i = 0 \qquad (3)$$

where $k^2_0 = \omega^2 \mu_0 \varepsilon_0$ while ω is the angular frequency, μ_0 and ε_0 are the permeability and permittivity of free space.

The Fourier integral solution of equation (3) given by [5] for Gaussian beam incident field is

$$E_z^i = \frac{E_0}{2k_0\sqrt{\pi}\beta} \int_{-\infty}^{\infty} exp\left[-\frac{\alpha^2}{4\beta^2} - j((x+x_0)\sqrt{k_0^2 - \alpha^2} - \alpha y)\right] d\alpha \qquad (4)$$

At evanescent region, the sign on the square root changes across the boundary $y' = 0$ as

$$\left. \begin{array}{l} \sqrt{k_0^2 - \alpha^2}, \quad |\alpha| \leq k_0, \\ -j\sqrt{k_0^2 - \alpha^2}, |\alpha| > k_0, y' \geq 0 \\ j\sqrt{k_0^2 - \alpha^2}, \quad |\alpha| > k_0, y' \leq 0 \end{array} \right\} \qquad (5)$$

By changing the variable of integration into an angular function as suggested in [6] by

$$\sin\theta = \frac{\alpha}{k_0} \qquad (6)$$

Then equation (4) becomes [8,12]

$$E_z^i = \frac{E_0}{2k_0\sqrt{\pi}\beta} \int_{-\frac{\pi}{2} - j\infty}^{\frac{\pi}{2} + j\infty} exp\left[-\frac{k_0^2 \sin^2\theta}{4\beta^2} - jk_0((x+x_0)\cos\theta + y\sin\theta)\right]\cos\theta \, d\theta \qquad (7)$$

Transformation from Cartesian coordinates (x, y, z) to cylindrical coordinates (ρ, ϕ, z) using relations: $x = \rho \cos\phi$, $y = \rho \sin\phi$ and $x_0 = \rho_0 \cos\phi_0$ yields

$$E_z^i = \frac{kE_0}{2\sqrt{\pi}\beta} \int_{-\frac{\pi}{2} - j\infty}^{\frac{\pi}{2} + j\infty} exp\left[-\frac{k_0^2 \sin^2\theta}{4\beta^2} - jk_0(\rho\cos(\phi - \theta) + \rho_0\cos\phi_0 \cos\theta)\right]\cos\theta \, d\theta \qquad (8)$$

The Gaussian beam may be expressed as sum of beams with TE and TM polarization.

2.1. Normal incident Gaussian beam: parallel polarization

Consider an incident Gaussian beam field on the PEMC cylinder with parallel polarization. It can be written in terms of cylindrical waves and weight functions as[18,19]

$$E_Z^i = E_0 \sum_{n=-\infty}^{\infty} j^{-n} J_n(k_0\rho) e^{jn\phi} A_n \qquad (9)$$

$$H_\rho^i = -\frac{E_0}{\omega\mu\rho} \sum_{n=-\infty}^{\infty} n j^{-n} J_n(k_0\rho) e^{jn\phi} A_n \qquad (10)$$

$$H_\phi^i = \frac{E_0}{j\eta_0} \sum_{n=-\infty}^{\infty} j^{-n} J_n'(k_0\rho) e^{jn\phi} A_n \qquad (11)$$

$$A_n = \frac{1}{2\sqrt{\pi}\beta} \int_{-\frac{\pi}{2} - j\infty}^{\frac{\pi}{2} + j\infty} exp\left[-\frac{k_0^2 \sin^2\theta}{4\beta^2} - jk_0(n\theta + \rho_0\cos\phi_0 \cos\theta)\right]\cos\theta \, d\theta \qquad (12)$$

The scattered fields can be written as

$$E_Z^s = E_0 \sum_{n=-\infty}^{\infty} j^{-n} a_n H_n^2(k_0\rho) e^{jn\phi} \qquad (13)$$

$$E_\rho^s = \frac{jn}{k_0\rho} H_n^2(k_0\rho) \sum_{n=-\infty}^{\infty} j^{-n} b_n H_n^2(k_0\rho) e^{jn\phi} \qquad (14)$$

$$E_\phi^s = -E_0 \sum_{n=-\infty}^{\infty} j^{-n} b_n H_n^{2'}(k_0\rho) e^{jn\phi} \qquad (15)$$

$$H_\rho^s = \frac{E_0}{\omega\mu\rho} \sum_{n=-\infty}^{\infty} n a_n j^{-n} H_n^2(k_0\rho) e^{jn\phi} \qquad (16)$$

$$H_\phi^s = -\frac{E_0}{j\eta_0} \sum_{n=-\infty}^{\infty} a_n j^{-n} H_n^{2'}(k_0\rho) e^{jn\phi} \qquad (17)$$

$$H_z^s = \frac{E_0}{j\eta_0} \sum_{n=-\infty}^{\infty} b_n j^{-n} H_n^2(k_0\rho) e^{jn\phi} \qquad (18)$$

where $H_n^2(.)$ is the Hankel function of the second kind, a_n is the scattering coefficient of the co polarized fields and b_n is the scattering coefficient of the crossed polarized fields.

2.2 Normal incident Gaussian beam: perpendicular polarization

The incident Gaussian beam field on the PEMC cylinder with perpendicular polarization can be written in terms of cylindrical waves and weight functions as[18,19]

$$E_\rho^i = -\frac{E_0}{\omega\mu\rho} \sum_{n=-\infty}^{\infty} n j^{-n} J_n(k_0\rho) e^{jn\phi} A_n \qquad (19)$$

$$E_\phi^i = \frac{E_0}{j\eta_0} \sum_{n=-\infty}^{\infty} j^{-n} J_n'(k_0\rho) e^{jn\phi} A_n \qquad (20)$$

$$H_Z^i = E_0 \sum_{n=-\infty}^{\infty} j^{-n} J_n(k_0\rho) e^{jn\phi} A_n \qquad (21)$$

The scattered fields are given by

$$H_Z^s = E_0 \sum_{n=-\infty}^{\infty} j^{-n} c_n H_n^2(k_0\rho) e^{jn\phi} \qquad (22)$$

$$H_\rho^s = \frac{jn}{k_0\rho} H_n^2(k_0\rho) \sum_{n=-\infty}^{\infty} j^{-n} d_n H_n^2(k_0\rho) e^{jn\phi} \qquad (23)$$

$$H_\phi^s = -E_0 \sum_{n=-\infty}^{\infty} j^{-n} d_n H_n^{2'}(k_0\rho) e^{jn\phi} \qquad (24)$$

$$E_\rho^s = \frac{E_0}{\omega\mu\rho} \sum_{n=-\infty}^{\infty} n c_n j^{-n} H_n^2(k_0\rho) e^{jn\phi} \qquad (25)$$

$$E_\phi^s = -\frac{E_0}{j\eta_0} \sum_{n=-\infty}^{\infty} c_n j^{-n} H_n^{2'}(k_0\rho) e^{jn\phi} \qquad (26)$$

$$E_z^s = \frac{E_0}{j\eta_0} \sum_{n=-\infty}^{\infty} d_n j^{-n} H_n^2(k_0\rho) e^{jn\phi} \qquad (27)$$

c_n is the scattering coefficient of the co polarized fields and d_n is the scattering coefficient of the crossed polarized fields for perpendicular polarization.

2.3. Applications of the boundary conditions

For tangential field components the boundary condition is [16]

$$H_t^i + M E_t^i + H_t^s + M E_t^s = 0 \qquad (28)$$

and the boundary condition for the radial field components is

$$\varepsilon_0 E_r^i - M \mu_0 H_r^i + \varepsilon_0 E_r^s - M \mu_0 H_r^s = 0 \qquad (29)$$

By applying the tangential boundary condition at $\rho = a$ on the above expanded fields, the co-polarized and cross-polarized scattering coefficients a_n and b_n are calculated and given as

$$a_n = -\frac{H_n(ka)J_n'(ka) + M\eta_0^2 J_n(ka)H_n'(ka)}{(1+M\eta_0^2)H_n(ka)H_n'(ka)} A_n \qquad (30)$$

$$b_n = \frac{2M\eta_0}{\pi ka(1+M\eta_0^2)H_n(ka)H_n'(ka)} A_n \qquad (31)$$

$$c_n = -\frac{J_n(ka)H_n'(ka) + M\eta_0^2 H_n(ka)J_n'(ka)}{(1+M\eta_0^2)H_n(ka)H_n'(ka)} A_n \qquad (32)$$

$$d_n = \frac{2M\eta_0}{\pi a(1+M\eta_0^2)H_n(ka)H_n'(ka)} A_n \qquad (33)$$

The above calculated scattering coefficients can also be obtained by applying the radial boundary conditions as in equation (29). By using these coefficients into equations (30) to (33), we can obtain expressions for the scattered fields and for the echo widths. The special case of a plane wave incidence can be obtained by taking $\beta = 0$ in the above analysis. This is equivalent to an infinite Gaussian beam for which the amplitudes of the beam expansion coefficients approach the value of one. The beam width coefficients A_n in the radiated field region at $|\alpha| \leq k_0$ or $|\sin\theta| \leq 1$ can be separated as

$$A_n^{rad} = \frac{k_0}{2\sqrt{\pi}\beta} \int_{-\frac{\pi}{2}}^{\frac{\pi}{2}} exp\left[-\frac{k_0^2 \sin^2\theta}{4\beta^2} - j(n\theta + k_0\rho_0 \cos\phi_0 \cos\theta)\right] \cos\theta \, d\theta \qquad (34)$$

The beam width coefficients A_n in the evanescent field region at $|\alpha| > k_0$ or $|\sin\theta| > 1$ can also be separated as [7]

$$A_n^{evan} = \frac{k_0}{2\sqrt{\pi}\beta} \left(\int_{\frac{\pi}{2}}^{\frac{\pi}{2}+j\infty} exp\left[-\frac{k_0^2 \sin^2\theta}{4\beta^2} - j(n\theta + k_0\rho_0 \cos\phi_0 \cos\theta)\right] \cos\theta \, d\theta + \int_{-\frac{\pi}{2}-j\infty}^{-\frac{\pi}{2}} exp\left[-\frac{k_0^2 \sin^2\theta}{4\beta^2} - j(n\theta + k_0\rho_0 \cos\phi_0 \cos\theta)\right] \cos\theta \, d\theta \right) \qquad (35)$$

By applying the transformation

$$\theta = \frac{\pi}{2} + jv,$$

$$\theta = -\frac{\pi}{2} - jv$$

With some equation simplifications, we obtain

$$A_n^{evan} \quad = \frac{k_0}{2\sqrt{\pi}\beta} \int_{\frac{\pi}{2}}^{\frac{\pi}{2}+j\infty} exp\left[-\frac{k_0^2 \sin^2 \theta}{4\beta^2}\right] \sinh(v) \begin{Bmatrix} j^{-n} \exp[nv - jk_0\rho_0 \sin\phi_0 \, \sin\theta \,] \\ +j^n \exp[-nv + jk_0\rho_0 \sin\phi_0 \, \sin\theta \,] \end{Bmatrix} \, dv \qquad (36)$$

The ratio of the total scattered power by the scatterer to the incident power per unit area is called the echo width and is simply given by[12]

$$\sigma = 2\pi\rho \frac{W^s}{W^i} = 2\pi\rho \frac{|E^s|^2}{|E^i|^2} \qquad (37)$$

3. Results and discussions

The numerical results are based on the above analytical expressions developed for the scattering of a Gaussian beam from a PEMC cylinder. The results are presented for both the radiative and the evanescent regions. It is assumed that the frequency of the source is 1 GHz. The radius of the PEMC cylinder is taken as $a = 0.3$. To check the validity of the presented analytical and numerical results, the echo width of the PEMC cylinder when $M\eta \to \infty$ with those for a PEC cylinder in [5] has been compared. Expressions in equations (30) and (32) of this paper yield equations (14) and (27) of [5] for the case when $M\eta \to \infty$. Investigations on the radar cross section RCS distribution with the scattering angle, radius of cylinder, admittance parameter, and the beam width, are explicated using equation (37) along with the scattering coefficients a_n and b_n from equations (30) and (31) for parallel polarization case and similarly with the scattering coefficients c_n and d_n for the perpendicular polarization case. Results for plane wave incidence are obtained using $k\beta = 0$.

Fig. 2 shows comparison of the field pattern of a Gaussian beam from a PEMC cylinder verses the scattering angle ϕ(degree) for $M\eta_0 = \infty$ and the Echo width using coefficients of equation (14) of [5] at beam with $\beta = 2.5$. It can be noted that the behavior of the field at $M\eta_0 = \infty$ (dotted line) corresponds to perfect electric conductor cylinder which is exactly the same when we plot with equation (14) of [5] (solid line).
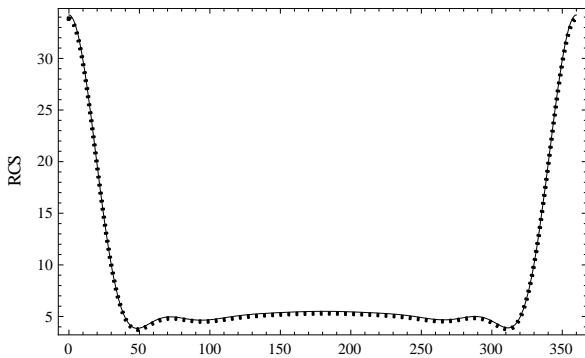
Fig. 2. Comparison of the field pattern of a Gaussian beam from a PEMC cylinder verses the scattering angle ϕ for $M\eta_0 = \infty$ (solid line) and the Echo width using coefficients of equation (14) of [5] (dotted line)at beam with $\beta = 2.5$.

Fig. 3 shows the comparison of RCS of a Gaussian beam from a PEMC cylinder into radiation region verses scattering angle ϕ for the co-polarized component with $ka = 0.3$ (solid line), $ka = 1$ (thick dotted line), $ka = 1.5$ (dashed line), $ka = 2$, (dotted line) and $ka = 3$ (thick solid line) at $\beta = 2.5$ and $M\eta_0 = 2.5$. Notable effects of radius of cylinder has been observed.
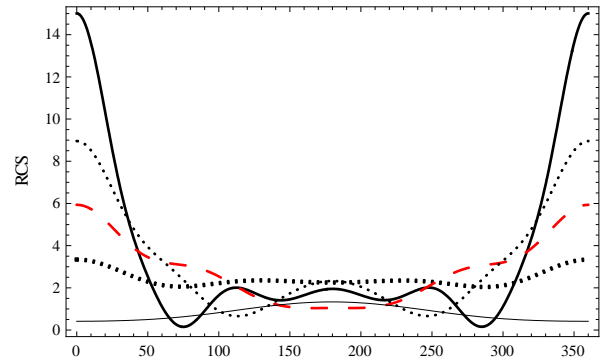
Fig. 3. Normalized bistatic RCS of a Gaussian beam from a PEMC cylinder into radiative region verses angle ϕ for the cross-polarized component with $ka = 0.3$ (solid line), $ka = 1$ (thick dotted), $ka = 1.5$ (dashed line), $ka = 2$ (dotted line), and $ka = 3$ (thick solid line).

Fig. 4 shows the comparison of RCS of a Gaussian beam from a PEMC cylinder into radiation region verses scattering angle ϕ(degree) for the co-polarized component with $M\eta_0 = 0$ (solid line), $M\eta_0 = 0.2$ (thick dotted line), $M\eta = 0.5$ (dashed line), $M\eta = 0.8$, (dotted line) and $M\eta_0 = 1$ (thick solid line). It is observed that intensity of the RCS increases with the increase of the value of the admittance parameter $M\eta_0$.
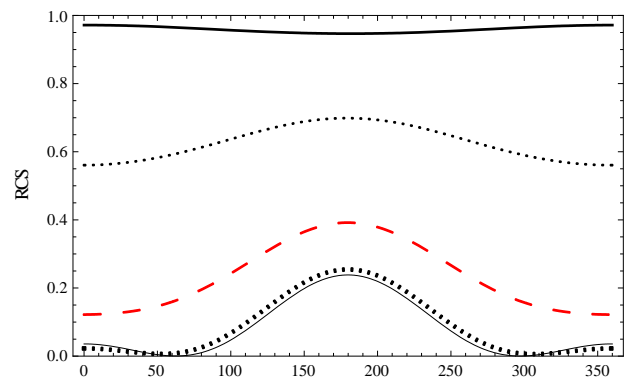
Fig. 4. Normalized bistatic RCS of a Gaussian beam from a PEMC cylinder in the radiation region verses angle ϕ for the cross-polarized component with $M\eta = 0$ (solid line), $M\eta = 0.2$ (thick dotted line), $M\eta = 0.5$ (dashed line), $M\eta = 0.8$ (dotted line), and $M\eta = 1$ (thick solid line).

Fig. 5 shows the comparison of the RCS of a PEMC cylinder from a Gaussian beam in the radiation region verses the scattering angle ϕ (degree) for the cross-polarized component with $M\eta_0 = 0$ (solid line), $M\eta_0 = 0.2$ (thick dotted line), $M\eta_0 = 0.5$ (dashed line), $M\eta = 0.8$, (dotted line) and $M\eta_0 = 1$ (thick solid line). It is observed that the cross components of the field disappear with higher value of admittance parameter $M\eta_0$ as expected.
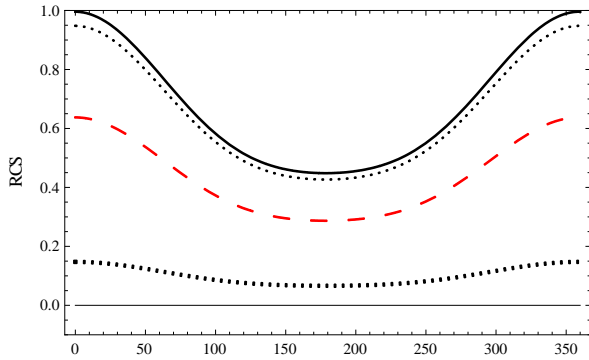
Fig. 5. Normalized bistatic RCS of a Gaussian beam from a PEMC cylinder in the radiation region verses ϕ for the co-polarized component with $M\eta = 0$ (solid line), $M\eta = 0.2$ (thick dotted line), $M\eta = 0.5$ (dashed line), $M\eta = 0.8$ (dotted line), and $M\eta = 1$ (thick solid line).

Fig. 6 and Fig. 7 show the comparison of the normalized bistatic echo of a Gaussian beam from a PEMC cylinder in the radiation region verses the scattering angle ϕ (degree) for the co-polarized and cross-polarized fields for $k\beta = 0$ (solid line), $k\beta = 12$ (thick dotted line), $k\beta = 13$ (dashed line), $k\beta = 14$ (dotted line) and $k\beta = 15$ (thick solid line) at $M\eta = 0.5$. It is observed that a simple incident plane wave can be obtained when $k\beta = 0$ and the infinitely wide Gaussian beam can be obtained when the amplitude of the expansion coefficients A_n approaches unity. From figure 6 shows that when incident wave changes from Gaussian beam to plane notable difference between amplitude is observed.
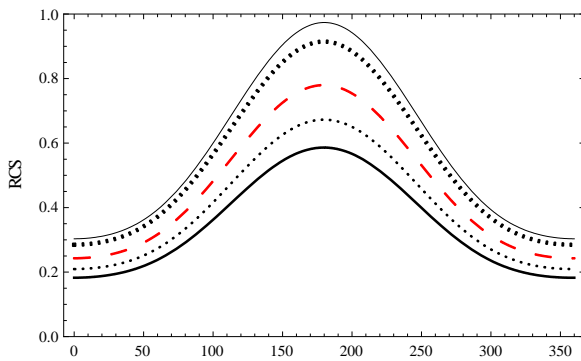
Fig. 6. Normalized bistatic RCS of a Gaussian beam from a PEMC cylinder into radiation region verses ϕ for the cross-polarized component with $k\beta = 0$ (solid line), $k\beta = 12$ (thick dotted line), $k\beta = 13$ (dashed line), $k\beta = 14$ (dotted line) and $k\beta = 15$ (thick solid line).
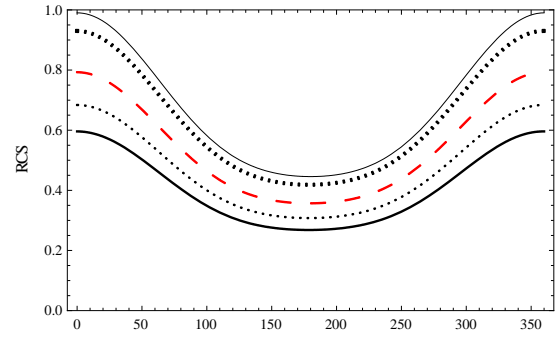
Fig. 7. Normalized bistatic RCS of a Gaussian beam from a PEMC cylinder in the radiation region verses ϕ for the co-polarized component with $k\beta = 0$ (solid line), $k\beta = 12$ (thick dotted line), $k\beta = 13$ (dashed line), $k\beta = 14$ (dotted line), and $k\beta = 15$(thick solid line) at $M\eta = 0.5$.

.

Fig. 8 and Fig. 9 show the normalized bistatic fields of a Gaussian beam from a PEMC cylinder in the evanescent region verses the scattering angle ϕ(degree) for the co-polarized and the cross-polarized components with $M\eta = 0$ (solid line), $M\eta = 0.2$ (thick dotted line), $M\eta = 0.5$ (dashed line), $M\eta = 0.8$, (dotted line) and $M\eta = 1$ (thick solid line) at $k\beta = 2.5$.
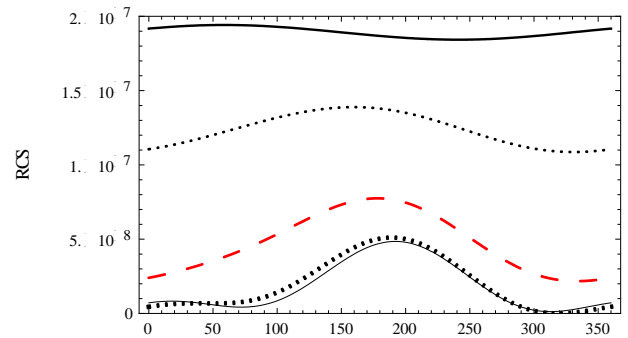
Fig. 8. Normalized bistatic RCS of a Gaussian beam from a PEMC cylinder in the evanescent region verses the scattering angle ϕ for the cross-polarized component with $M\eta = 0$(solid line), $M\eta = 0.2$(thick dotted line), $M\eta = 0.5$ (das hed line), $M\eta = 0.8$ (dotted line), and $M\eta = 1$ (thick solid line).
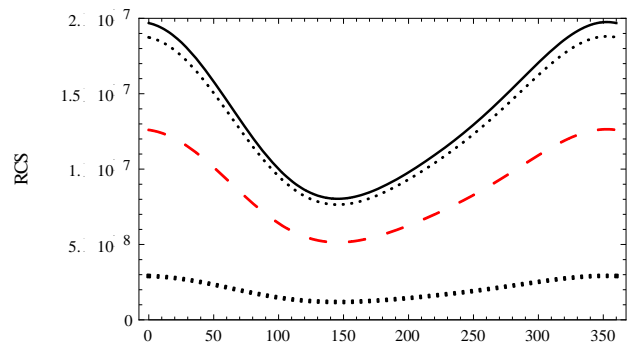
Fig. 9. Normalized bistatic RCS of a Gaussian beam from a PEMC cylinder in the evanescent region verses ϕ for the co-polarized component with $M\eta = 0$ (solid line), $M\eta = 0.2$ (thick dotted line), $M\eta = 0.5$ (dashed line), $M\eta = 0.8$ (dotted line), and $M\eta = 1$ (thick solid line).

Fig. 10 and Fig. 11 show the normalized bistatic fields of a Gaussian beam from a PEMC cylinder in the evanescent region verses the scattering angle ϕ for the cross-polarized component for $k\beta = 0$ (solid line), $k\beta = 12$ (thick dotted line), $k\beta = 13$ (dashed line), $k\beta = 14$ (dotted line), and $k\beta = 15$ (thick solid line) at $M\eta = 0.5$. It is observed from Figs. 8 to 11 that the evanescent waves may be converted to radiation. This conversion of evanescent waves into radiation can have applications for microwave source resolution to get imaging beyond the diffraction limit and, hence, it may be the basis for scanning optical microscopy.
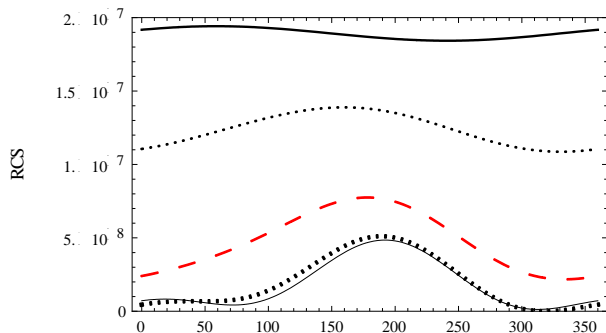
Fig. 10. Normalized bistatic RCS of a Gaussian beam from a PEMC cylinder into evanescent region verses ϕ for the cross-polarized component with $k\beta = 0$(solid line), $k\beta = 12$ (thick dott line), $k\beta = 13$(dash line), $k\beta = 14$ (dotted line) and $k\beta = 15$ (thick solid line) at $M\eta = 0.5$
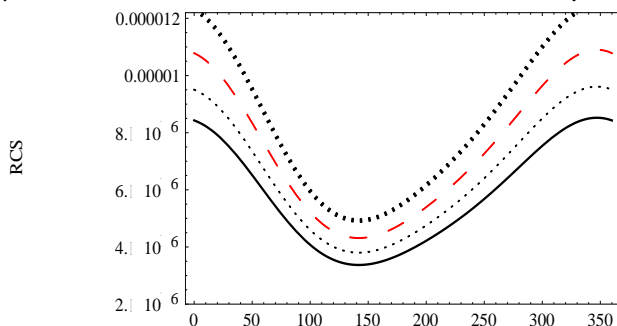
Fig. 11. Normalized bistatic RCS of a Gaussian beam from a PEMC cylinder in the evanescent region verses angle ϕ for the co-polarized component with $k\beta = 0$ (solid line), $k\beta = 12$ (thick dotted line), $k\beta = 13$ (dashed line), $k\beta = 14$ (dotted line), and $k\beta = 15$ (thick solid line).

4. Conclusions

Analysis for the electromagnetic scattering of a Gaussian beam by a PEMC cylinder including the evanescent region fields is effectively obtained in this paper contribution. Far scattering field patterns from the PEMC cylinder is determined by the admittance parameter, scattering angle, radius of cylinder and the incident beam width as described in this paper results. It is found that field patterns for incident Gaussian beam basically have same form like that of the plane wave

incidence. However the amplitude of field behavior obtained by plane wave expansion incident is larger than by using Gaussian beam incident. It is conclude from discussion concluded that an evanescent wave scatters from PEMC cylinder may be partially converted into radiation. This paper contribution can be easily extended to other emerging scattering problems such as scattering from multiple PEMC cylinders in complex media.

References

[1] F. D. Fornel, Evanescent waves from Newtonian optics to atomic optics, Springer Verlag, 2001.
[2] D. Courjon, Near field microscopy and near field optics, Imperial College Press, 2003.
[3] G. S.Smith, L. E. R. Petersson, IEEE Transactions on Antennas and Propagation, **48,** 1295 (2000).
[4] A. Z. Elsherbeni, G. Tian, M. Hamid, IEEE Proceeding, **2,** 542 (1992).
[5] S. Kozaki, IEEE, Transactions Antennas Propagation, **30,** 881(1982).
[6] S. Kozaki, IEEE, Transactions Antennas Propagation, **31,** 795 (1983).
[7] C. L. Li, C. H. Sun, C. C. Chiu, L. F. Tuen, C. H. Su, International Journal of Applied Electromagnetics and Mechanics, **42**, 349 (2009).
[8] P. Pawliuk, M. Yedlin, Journal of Optical Society of America A, **28,** 1177 (2011).
[9] Li H-Y, Li Q, Xia Z-W, Chinese Journal of Lasers, **39,** (2012).
[10] L. H-Y, L. Q, Xia Z-W, De-Y. Chen, Q. Wang, J. Infrared Milli Terahz Waves, **34,** 88 (2013).
[11] Li H-Y, Li Q, Xia Z-W, De-Y. Chen , Q. Wang, J. Infrared Milli Terahz Waves, **34,** 289 (2013).
[12] P. Pawliuk, M. Yedlin, Journal of Optical Society of America A, **26,** 2558 (2009).
[13] P. Pawliuk, M. Yedlin, Applied Physics B, DOI 10.1007/s00340-013-5534-y, (2013).
[14] I. V. Lindell, A. H. Shivola, IEEE Transactions on Antennas Propagation, **53,** 3012 (2005).
[15] I. V. Lindell, A. H. Sihvola, IEEE Transactions Antennas Propagation, **54,** 2553 (2006).
[16] R. Ruppin, Journal of Electromagnetic Waves and Applications, **20,** 1853 (2006).
[17] A. K. Hamid, F. R. Cooray, International Journal of Applied Electromagnetics and Mechanics, **38,** 1 (2012).
[18] S. Ahmad, Q. A. Naqvi, Optics Communication, **281,** 5664 (2008).
[19] S. Ahmad, Q. A. Naqvi, Progress in Electromagnetics Research, **78,** 25 (2008).

*Corresponding author: aghaffar@ksu.edu.sa;
                                 majeed@ksu.edu.sa